Available online at www.sciencedirect.com
SCIENCE DIRECT®
Solid-State Electronics 48 (2004) 207–215
SOLID-STATE ELECTRONICS
www.elsevier.com/locate/sse

Base transit time of graded-base Si/SiGe HBTs considering recombination lifetime and velocity saturation

S.T. Chang [a], C.W. Liu [b,*], S.C. Lu [c]

[a] Department of Electronic Engineering, Chung Yuan Christian University, Chungli 320, Taiwan, ROC
[b] Department of Electrical Engineering, Graduate Institute of Electronics Engineering, National Taiwan University, Taipei 106, Taiwan, ROC
[c] Electronic Research and Service Organization, Industrial Technology Research Institute, Hsinchu 300, Taiwan, ROC

Received 26 December 2001; accepted 12 January 2003

Abstract

The base transit time of Si/SiGe heterojunction bipolar transistor is analyzed including the effects of minority carrier recombination lifetime and velocity saturation. The reduction of recombination lifetime in the neutral base region increases the base transit time as compared to the infinite recombination lifetime, and the finite saturation velocity also degrades the base transit time, as compared to the infinite saturation velocity. This analytical analysis can obtain the optimum design of Ge profiles in the base to minimize the base transit time. The extremely heavy doping of the base can degrade the base transit time significantly if the base width is larger than the diffusion length.

Keywords: Base transit time; Minority carrier recombination lifetime; Velocity saturation; SiGe HBTs

1. Introduction

Since the first Si/SiGe heterojunction bipolar transistor (HBT) was reported in 1988 [1], the tremendous progress of Si/SiGe HBTs has been reached to have a maximum oscillation frequency of 285 GHz [2], a cut-off frequency of 350 GHz [3], and circuit applications on wireless [4] and optical communication [5]. The narrow-bandgap of SiGe allows heavy doping in the base with a concentration up to 2×10^{20} cm^{-3} [6], which significantly reduces the base resistance and hence increases the maximum oscillation frequency, as compared to the conventional Si bipolar junction transistors. However, the defects such as oxygen, SiC precipitates, dislocation, and the impurities in the heavily doped SiGe(C) base decrease the minority carrier recombination lifetime (T_n), and affect the base transit time, which is a major component of the cut-off frequency. Note that the reported recombination lifetime of SiGe base was widely scattered from 10^{-13} to 10^{-9} s probably due to different amount of defects in the base [7–9]. By neglecting the effects of recombination lifetime and velocity saturation, Kroemer's model gave an integral expression of the base transit time [10]. Suzuki and Nakayama modified the Kroemer's expression by taking finite saturation velocity into account [11]. Mohammadi derived a complex integral expression by considering recombination lifetime but neglecting velocity saturation [12]. Cressler et al. [13,14] derived a simple analytical expression for trapezoidal Ge profile based on Kroemer's model. Recently, Patri and Kumar have used Suzuki's model to study the optimal Ge profile to minimize the base transit time in SiGe HBTs [15,16]. In this paper, we derive an analytical expression for the base transit time based on the minority carrier continuity equation considering both finite recombination lifetime and finite saturation velocity. The design of optimal Ge profile to minimize the base transit time can be obtained by this model. The base structure for optimization has a linear ramp over the

* Corresponding author. Tel.: +886-2-2363-5251x515; fax: +886-2-2363-8247.
E-mail address: chee@cc.ee.ntu.edu.tw (C.W. Liu).

0038-1101/$ - see front matter © 2003 Elsevier Ltd. All rights reserved.
doi:10.1016/S0038-1101(03)00325-3

central portion of the base, similar to Winterton's structures [17,18], and this Ge profile has been also used in the Si/SiGe HBT fabrication [19].

2. Theory

The neutral base width (W) of 50 nm and uniform doping (N_B) is used in the analysis. In order to facilitate derivation of analytical model for the base transit time, it is necessary to make a judicious choice of models for the base transport parameters such as minority carrier mobility, effective intrinsic carrier concentration, minority carrier recombination lifetime.

The low-field minority electron mobility in Si is modeled using Swirhum's impurity–concentration-dependent minority electron mobility model [20,21]. The minority electron mobility in the strained SiGe films has been reported to be higher than that for Si. The mobility model in the SiGe base used in our analysis is as follows [15,22]:

$$\mu_{n,\mathrm{SiGe}}(0) = [1 + C \cdot \mathrm{Ge}]\mu_{n,\mathrm{Si}}(0) \tag{1}$$

where $\mu_{n,\mathrm{SiGe}}(0)$ is the low field minority electron mobility in SiGe, $\mu_{n,\mathrm{Si}}(0)$ is the low field minority electron mobility in Si, Ge is germanium mole fraction, and $C(=3)$ is a parameter obtained from Ref. [15]. For simplicity, the average mobility is used in graded Ge region. For a two-graded Ge profile as shown in Fig. 1, the average Ge in two region (I, II) are

$$\mathrm{Ge_I} = \mathrm{Ge}(X_T)/2 \quad \text{and} \quad \mathrm{Ge_{II}} = (\mathrm{Ge}(\mathrm{X_T}) + \mathrm{Ge}(\mathrm{W}))/2 \tag{2}$$

where W is neutral base width and X_T is as indicated in Fig. 1 (curve (a)). The field dependence of minority carrier mobility is taken into account using a modified Caughey–Thomas electric field dependent mobility model [23].

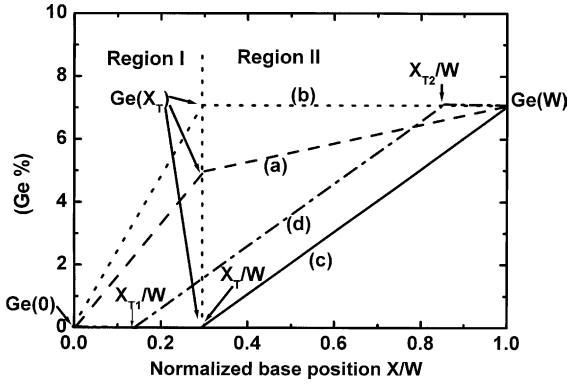

Fig. 1. The Ge profiles in the base used in our analysis: (a) two-graded region Ge profile, (b) trapezoidal Ge profile, (c) shift-triangle Ge profile, and (d) central-graded Ge profile.

$$\mu_{n\mathrm{SiGe}}(|E|) = \frac{\mu_{n\mathrm{SiGe}}(0)}{\left[1 + \left(\frac{\mu_{n\mathrm{SiGe}}(0)|E|}{v_s}\right)^{\beta}\right]^{\frac{1}{\beta}}} \tag{3}$$

where $\mu_{n\mathrm{SiGe}}(0)$ is low-field electron mobility obtained from Eq. (1), $\beta = 2$ for electron, v_s saturation velocity of electron in SiGe base, and

$$|E| = \frac{kT}{q}\left\{\frac{1}{n_{ie}^2(x)}\frac{\partial n_{ie}^2(x)}{\partial x}\right\} = \frac{\partial}{\partial x}\left\{\frac{\Delta E_{g,\mathrm{Ge}}(x)}{q}\right\} \tag{4}$$

In Eq. (4), the position-dependent effective intrinsic carrier concentration $n_{ie}(x)$ is modeled as

$$n_{ie}^2(x) = \gamma n_{ioSi}^2 \exp\left(\frac{\Delta E_{g,\mathrm{eff}}(x)}{kT}\right) \tag{5}$$

where γ is the ratio of effective density of states in SiGe base to that of silicon, n_{ioSi}, is the intrinsic carrier concentration in undoped silicon, and $\Delta E_{g,\mathrm{eff}}(x)$ is the effective bandgap reduction in the SiGe base.

$$\Delta E_{g,\mathrm{eff}}(x) = \Delta E_{g,\mathrm{HD}}(x) + \Delta E_{g,\mathrm{Ge}}(x) \tag{6}$$

where $\Delta E_{g,\mathrm{Ge}}(x)$ is the bandgap narrowing due to the presence of Ge, which is assumed to have a linear dependence on Ge concentration [24]. In the present study, the bandgap narrowing due to heavy doping effect, $\Delta E_{g,\mathrm{HD}}(x)$, is assumed to be identical to that of silicon. An approximation of the Slotboom-de Graff bandgap narrowing model [25] is used in our simulation

$$\Delta E_{g,\mathrm{HD}}(x) = E_0 \ln\left(\frac{N_B(x)}{N_1}\right) \tag{7}$$

with $E_0 = 18$ meV and $N_1 = 10^{17}$ cm^{-3}. The bandgap narrowing, $\Delta E_{g,\mathrm{Ge}}(x)$, in a two linear graded regions of the base (curve (a) in Fig. 1) is given by

$$\begin{aligned}\Delta E_{g,\mathrm{Ge}}(x) &= A_1[\mathrm{Ge}(X_T) - \mathrm{Ge}(0)]x/X_T \\ &\quad + A_1\mathrm{Ge}(0) \quad 0 \leqslant x \leqslant X_T \\ \Delta E_{g,\mathrm{Ge}}(x) &= A_1[\mathrm{Ge}(W) - \mathrm{Ge}(X_T)](x - X_T)/(W - X_T) \\ &\quad + A_1\mathrm{Ge}(X_T) \quad X_T \leqslant x \leqslant W\end{aligned} \tag{8}$$

where $A_1 = 740$ meV, $\mathrm{Ge}(X_T)$ is the Ge concentration at X_T, $\mathrm{Ge}(W)$ is Ge concentration at $x = W$, and W is neutral base width. The typical value of electron saturation velocity is $\sim 10^7$ cm/s for Si and $\sim 6\times 10^6$ cm/s for Ge. The dependence of saturation velocity on Ge content is given by [26,27]

$$v_s(\mathrm{Ge}) = v_s(0)\frac{C_2}{C_2 + \mathrm{Ge}(1 - \mathrm{Ge})} \tag{9}$$

where $v_s(0)$ is the saturation velocity for pure silicon, Ge is germanium mole fraction, and $C_2 = 0.342$.

Fig. 2 shows Klaassen's model of experimentally measured minority electron lifetime for p-type Si. The

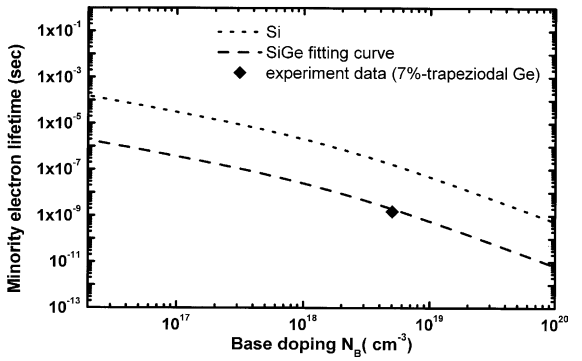

Fig. 2. Recombination lifetime vs base doping for Si and SiGe.

experimental value of recombination lifetime is 1.5 ns in p-type 7%-trapezoidal SiGe base with $N_B = 5 \times 10^{18}$ cm^{-3} [7]. The SiGe lifetime is scaled by shifting the Si curve downward to this experimental data point. The smaller recombination lifetime in SiGe than that in Si is probably caused by oxygen level, dislocations, doping level, and other point defects such as SiC precipitates during growth. Due to lack of enough experimental results to model Ge dependence of lifetime, the reduction of lifetime is simplistically assumed the same at a fixed base doing N_B for all Ge profile in our calculation.

The electron current density J_n for base doping concentration N_B is given by [28]

$$J_n = qD_n \frac{dn(x)}{dx} + q\mu_n E(x) n(x) \tag{10}$$

To determine minority carrier concentration $n(x)$, the continuity equation for electron is used

$$\Delta \cdot J_n = \frac{q\Delta n}{\tau_n} \tag{11}$$

where $\Delta n = n - n_0$, $n_0 = n_{ie}^2(x)/N_B$.

Combining (11) and (12), then the differential equation can be shown to be

$$\frac{d^2 n}{dx^2} - \frac{\mu_n E}{D_n}\frac{dn}{dx} - \frac{n}{L_n^2} = -\left(\frac{n_0}{L_n^2}\right) \tag{12}$$

In the linear-graded region of the base, the electric field E is constant in Eq. (12), and $n(x)$ can be solved analytically.

$$\begin{aligned} n_I(x) &= Ae^{r_+ x} + Be^{r_- x} + Ge^{\alpha_1 x} \quad 0 < x < X_T \\ n_{II}(x) &= Ce^{r'_+(x-X_T)} + De^{r'_-(x-X_T)} \\ &\quad + G_T e^{\alpha_2 (x-X_T)} \quad X_T < x < W \\ r_\pm &= \left[\alpha_1 \pm \sqrt{\alpha_1^2 + 4\beta_1}\right] \Big/ 2, \\ r'_\pm &= \left[\alpha_2 \pm \sqrt{\alpha_2^2 + 4\beta_2}\right] \Big/ 2 \end{aligned} \tag{13}$$

where $\alpha_1 = \mu_{n1} E_1 / D_{n1}$, $\alpha_2 = \mu_{n2} E_2 / D_{n2}$, $E_1 = E_{g,Grade}/X_T$, $E_2 = E_{g,Grade1}/(W - X_T)$, $G = (n_{ie}^2(0)/N_B)e^{E_g(0)/kT}$, $G_T = (n_{ie}^2(0)/N_B)e^{E_g(X_T)/kT}$, $E_{g,Grade} = \Delta E_{g,Ge}(X_T) - \Delta E_{g,Ge}(0)$, $E_{g,Grade1} = \Delta E_{g,Ge}(W) - \Delta E_{g,Ge}(X_T)$, $D_{n1,2}$ is the diffusion coefficient, and $\mu_{n1,2}$ is the minority electron mobility. The subscripts 1 and 2 indicate regions I and II, respectively. The coefficients in Eq. (13) are determined by the following boundary conditions and are given in Appendix A. $n(0)$ is expressed as

$$n(0) = \frac{n_{ie}^2(0)}{N_B} e^{(qV_{BE}/kT)} \tag{14}$$

We assume that the electric field at the base–collector junction is large enough to saturate the electron velocity. Thus, electron can be moved at the saturation velocity at edge of the depletion layer. Assuming that the electron velocity in the base–collector depletion region saturates at v_s, $n(W)$ is expressed as

$$n(W) = \frac{-J_n(W)}{qv_s} \tag{15}$$

At the interface between regions I and II, the electron concentration and the total current (the sum of diffusion and drift current) are continuous

$$\begin{aligned} n_I(X_T) &= n_{II}(X_T) \\ J_{nI}(X_T) &= J_{nII}(X_T) \end{aligned} \tag{16}$$

The base transit time is given by

$$\tau_B = \frac{-q\int_0^W n(x)\,dx}{J_n(W)} \tag{17}$$

After solving $n(x)$ and $J_n(W)$, Eq. (17) is expressed in the analytical form as

$$\tau_B = \frac{-\left[\frac{A}{r_+}(e^{r_+ X_T} - 1) + \frac{B}{r_-}(e^{r_- X_T} - 1) + \frac{G}{\alpha_1}(e^{\alpha_1 X_T} - 1) + \frac{C}{r'_+}(e^{r'_+ X_T} - 1) + \frac{D}{r'_-}(e^{r'_- X_T} - 1) + \frac{G}{\alpha_2}(e^{\alpha_2 X_T} - 1)\right]}{D_{n2}\left(Cr'_+ e^{r'_+(W-X_T)} + Dr'_- e^{r'_-(W-X_T)} + G_T \alpha_2 e^{\alpha_2(W-X_T)}\right) - \mu_{n2} E_2 \left(Ce^{r'_+(W-X_T)} + De^{r'_-(W-X_T)} + G_T e^{\alpha_2(W-X_T)}\right)} \tag{18}$$

The results are applied to the base with two linearly graded Ge regions, and similar analysis can be performed in three-graded or multi-graded Ge profiles.

A different definition of base transit time (the average time for traversing the base) is used in literatures [12,16].

$$\tau'_{\mathrm{B}} = -q \int_0^W \frac{n(x)\,\mathrm{d}x}{J_n(x)} \tag{19}$$

Comparison between Eq. (18) and (19) shows that the both base transit times are the same if recombination is negligible in the base region. For serious recombination, these two transit times are different and will be addressed in Section 3.

Recently, many studies on optimal Ge profile for SiGe base HBTs have reported [17,18]. These studies attempt to find an optimal Ge profile to minimize the base transit time. Two kinds of constraints have been used in the optimum design of the Ge profile: fixed Ge content at base collector junction and constant integral Ge content in the base. Winterton et al. [17] used an iterative procedure to find out the optimal Ge profile considering both constraints. Rinaldi et al. [18] used the method based on the maximum principle to obtain the optimal Ge profiles for both conditions. The former constraint is adopted in our simulation, but similar analysis can also be applied to the constraint of constant integral Ge content in the base. Note that the constraint with constant Ge content at base–collector junction can be easily implemented using either the rapid thermal chemical vapor deposition or ultrahigh vacuum chemical vapor deposition.

3. Results and discussion

3.1. Base transit time

The base transit time versus recombination lifetime for two different definitions of base transit time are shown in Fig. 3. For recombination lifetime $\gtrsim 0.1$ ns, both base transit times slightly increase as recombination lifetime decreases. For recombination lifetime $\gtrsim 0.1$ ns, τ_{B} increases with decreasing recombination lifetime, while τ'_{B} decreases with decreasing recombination lifetime.

According to Mohammadi's explanation [12], when recombination lifetime decreases, the minority electron stored in the base decreases, and thus the base transit time decreases. However, the effect that collector current also decreases as the recombination lifetime decreased has to be taken into account. In the exact expression of Eq. (18), both effects are taken into account, and the base transit time increases as the recombination lifetime decreases. Eq. (18) will be used in our following simulation.

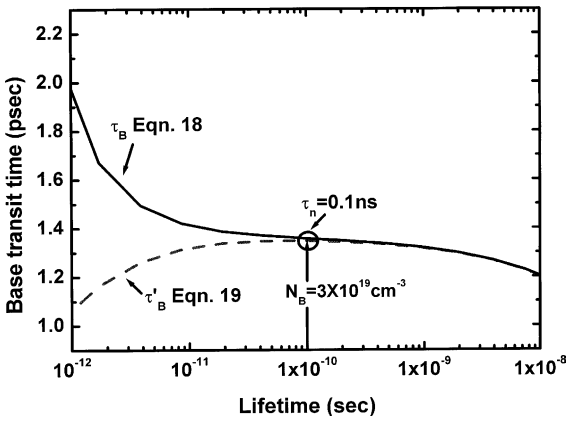

Fig. 3. The base transit time vs recombination lifetime for two different definitions of base transit time. The trapezoidal Ge profile (i.e. $\mathrm{Ge}(0) = 0\%$, $\mathrm{Ge}(X_T) = \mathrm{Ge}(W) = 7\%$, and $X_T/W = 0.88$) and base width of 50 nm are used in calculation.

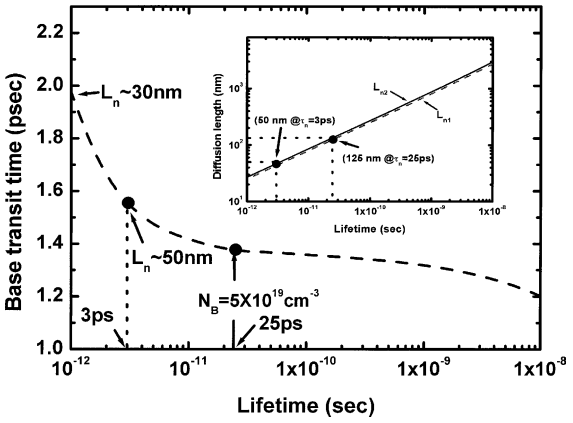

Fig. 4. The base transit time vs minority carrier recombination lifetime. The relation between diffusion length and recombination is shown in the inset. L_{n1} and L_{n2} are the diffusion lengths in the linear region (I) and the flat region (II) of trapezoidal Ge profile, respectively.

Fig. 4 shows the sensitivity of base transit time to the minority carrier recombination lifetime. This result is obtained by using trapezoidal Ge profile as shown in the curve (b) of Fig. 1 (i.e. $\mathrm{Ge}(W) = 7\%$, $\mathrm{Ge}(X_T) = 7\%$, $X_T/W = 0.88$). The relation between diffusion length and recombination lifetime is shown in the inset. L_{n1} and L_{n2} are the diffusion lengths in the linear region (I) and the flat region (II) of trapezoidal Ge profile, respectively. The other two types of Ge profiles have similar results. The decrease of base recombination lifetime due to the increasing base doping reduces electron mobility. The decreasing mobility slightly increases base transit time down to the recombination lifetime of 25 ps, and the

base transit time start to increase rapidly for the recombination lifetime shorter than 25 ps (corresponding diffusion length = 125 nm = 0.4 W). At the recombination lifetime of 1 ps, the diffusion length (~30 nm) is smaller than base width (50 nm). Note that the diffusion length is 50 nm at the lifetime of 3 ps. Most electrons injected from the emitter recombine with holes in the base, and cannot reach the collector. The transistor does not operate normally. The extremely low recombination lifetime (i.e., defective base) requires smaller base width than diffusion length without degrading the base transit time. We use $\tau_n = 2.5 \times 10^{-11}$ s for $N_B = 5 \times 10^{19}$ cm^{-3} (diffusion length ~125 nm) in the following simulation.

Three types of Ge profiles, two-graded region, trapezoid, and shift triangle (Fig. 1(a), (b), and (c)), are used to investigate the base transit time by considering both finite recombination lifetime and finite saturation velocity. The Ge content at base–collector junction is fixed at 7% in analysis. Table 1 shows the numerical results of injected electron current at collector junction $J_n(W)$, stored electron charge, and base transit time for three different Ge profiles in the base under four different conditions: (1) τ_n = infinite and v_s = infinite, (2) τ_n = infinite and $v_s = 8.2 \times 10^6$ cm/s, (3) $\tau_n = 2.5 \times 10^{-11}$ s and v_s = infinite, and (4) $\tau_n = 2.5 \times 10^{-11}$ s and $v_s = 8.2 \times 10^6$ cm/s. The effect of finite recombination lifetime is to decrease $J_n(W)$ and to reduce the stored electron charge in the base for all three Ge profiles. The curves (1) and (2) of Fig. 5, corresponding to conditions (1) and (2), show the steeper electron concentration profile at base–collector junction due to infinite recombination lifetime for trapezoidal Ge profile, as compared with curve (3) and (4). The other two types of Ge profiles have the similar results. Since electrons can recombine with holes by the finite recombination lifetime, both the stored electron charge in the base and collector current at base–collector junction $J_n(W)$ decrease, as compared to infinite recombination lifetime. As a numerical result, the base transit time which is the ratio of stored electron charge to $J_n(W)$ increases due to the finite recombination lifetime.

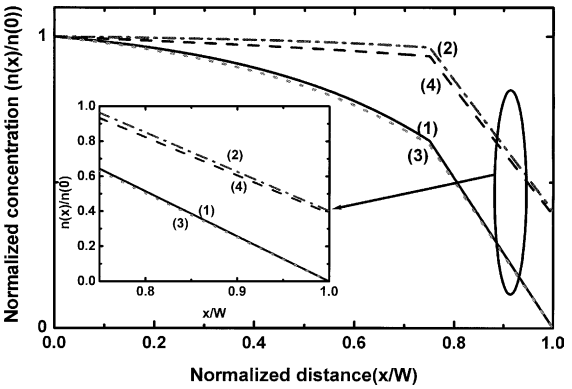

Fig. 5. Normalized electron concentration profile in trapezoidal Ge profile under four different conditions: (1) τ_n = infinite and v_s = infinite (solid line), (2) τ_n = infinite and $v_s = 8.2 \times 10^6$ cm/s (dash dot line), (3) $\tau_n = 2.5 \times 10^{-11}$ s and v_s = infinite (dot line), and (4) $\tau_n = 2.5 \times 10^{-11}$ s and $v_s = 8.2 \times 10^6$ cm/s (dash line). The optimal $X_T/W = 0.75$ in trapezoidal Ge profile is used in the calculation.

The effects of finite saturation velocity decreases $J_n(W)$ and increases the stored electron charge in the base for all three Ge profiles (Table 1). The finite saturation velocity leads to the accumulation of electron concentration at base–collector junction, and thus the slope of the electron profiles at base–collector junction are smoother (curves (2) and (4) of Fig. 5, corresponding to conditions (2) and (4)). The diffusion current decreases as compared to infinite saturation velocity. The accumulation of electron in base–collector junction also increases the stored electron charge. Therefore, the base transit time increases due to finite saturation velocity.

Fig. 6(a) shows the variation of the base transit time with X_T/W of trapezoidal Ge profile in the base under above four conditions. The optimal value of X_T/W for all four conditions are about 0.75–0.95. It is clear that finite recombination lifetime can increases the base transit time, and the finite saturation velocity also increases the base transit time for all value of X_T as

Table 1
The numerical results of SiGe HBT with various base structures

Ge profile	Trapezoidal ($X_T/W = 0.75$)				Shift triangle ($X_T/W = 0.17$)				Two graded ($X_T/W = 0.58$)			
Condition	(1)	(2)	(3)	(4)	(1)	(2)	(3)	(4)	(1)	(2)	(3)	(4)
$J_n(W)$ (A/cm^2)	98.95	86.42	96.63	83.51	64.28	59.01	62.87	57.27	90.49	80.61	88.37	78.02
Stored electron ($\times 10^{-11}$ c/cm^2)	9.68	11.95	9.55	11.70	6.53	7.79	6.46	7.67	9.27	11.08	9.15	10.87
Base transit time τ_B (ps)	0.97	1.38	0.99	1.40	1.01	1.32	1.03	1.34	1.02	1.37	1.03	1.39

The four conditions used in the calculations are: (1) τ_n = infinite and v_s = infinite, (2) τ_n = infinite and $v_s = 8.2 \times 10^6$ cm/s, (3) $\tau_n = 2.5 \times 10^{-11}$ s and v_s = infinite, and (4) $\tau_n = 2.5 \times 10^{-11}$ s and $v_s = 8.2 \times 10^6$ cm/s.

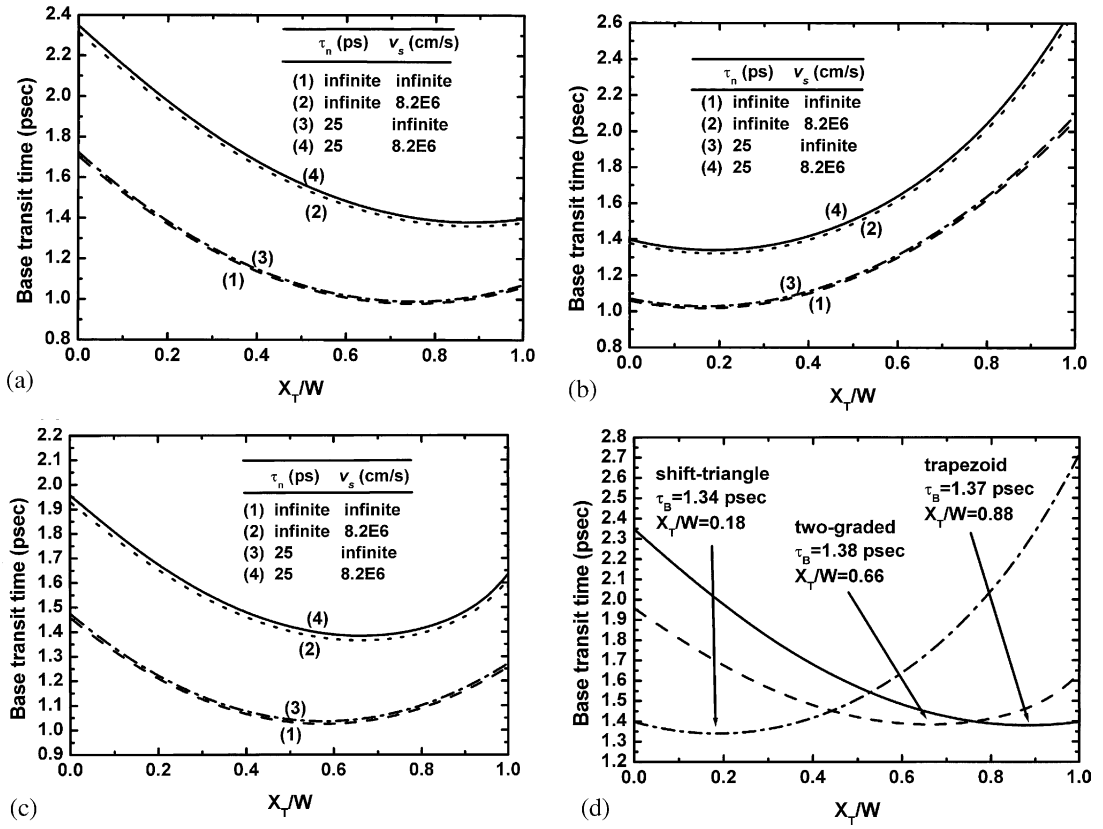

Fig. 6. The base transit time vs X_T/W of: (a) trapezoidal, (b) shift triangle, and (c) two graded Ge profile in base under the same conditions in Fig. 5(d). The base transit time vs X_T/W for three Ge profiles under the condition (4).

compared to the ideal conditions at optimal value of X_T/W, the finite lifetime increases base transit time slightly about 1%, the finite saturation velocity increases base transit time about 39%, and both lifetime and saturation velocity increase base transit time about 41%. The effect of finite saturation velocity is to move the position of optimal X_T/W toward the base collector junction slightly, and the effect of finite recombination lifetime does not change the position of optimal X_T/W significantly. The shift-triangle and two-graded Ge profiles have the similar results as shown in Fig. 6(b) and (c), respectively. The optimal value of X_T/W in shift-triangle Ge profile is approximately 0.17–0.2, close to emitter–base junction, and the optimal values of X_T/W in two-graded Ge profile under four conditions are approximately 0.5. For shift-triangle and two-graded Ge profile, the finite lifetime increases base transit time ~1% and ~1%, the finite saturation velocity increases base transit time ~29% and ~33%, and both lifetime and saturation velocity increase base transit time ~31% and ~35%, respectively. Fig. 6(d) shows that shift triangle Ge profile has the smallest base transit time among all three Ge profiles under the condition (4). Similar results are obtained for the other three conditions. This indicates that the electric field in the central base is the most effective way to reduce the base transit time.

3.2. Ge profile design consideration

For the constraint with Ge concentration fixed at base–collector junction, Winterton et al. [17] demonstrated that the central graded Ge profile is the optimal profile for base transit time by using an iterative method. Similar results are reported by Rinaldi et al. [18]. The central graded Ge profile shown in Fig. 1(d) is adopted in our optimization to find the optimal value of (X_{T1}/W, X_{T2}/W). In this profile, the drift field is at the central base, since the central field is the most effective to decrease the base transit time as shown in Section 3.1. For given three values of X_{T1}/W (0, 0.2, 0.35), the base transit time vs X_{T2}/W is shown in Fig. 7. The optimal position of X_{T2}/W is around 0.75–0.88 for different values of X_{T1}/W. The optimal value of X_{T2}/W and minimum base transit time for different given value of X_{T1}/W are shown in the inset of Fig. 7. It is clear that the optimal X_{T1}/W is ~0.20 and optimal X_{T2}/W is ~0.82.

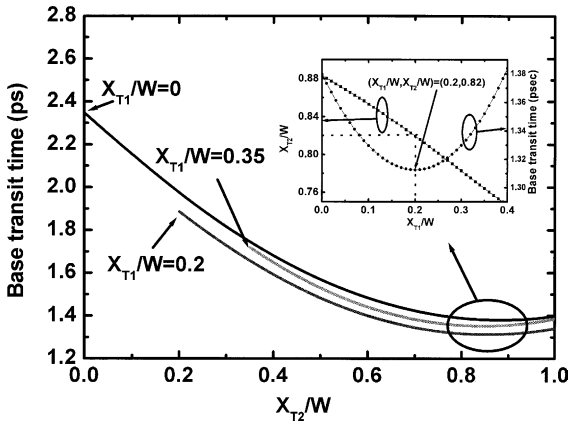

Fig. 7. Base transit time vs X_{T2}/W for three different values of X_{T1}/W of a central-graded Ge profile in the base. The Ge profile is shown in the curve (d) of Fig. 1. The inset shows base transit time and optimum value of X_{T2}/W vs X_{T1}/W.

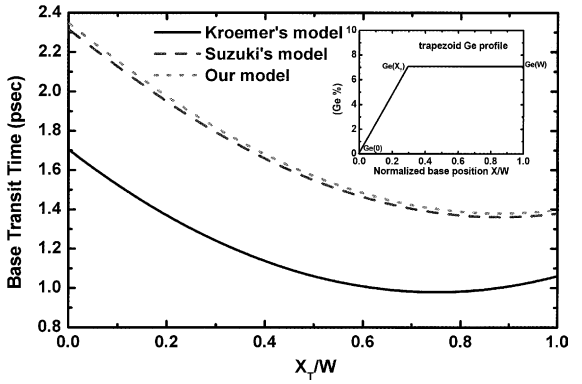

Fig. 8. Comparison between our model, Kroemer's model, and Suzuki's model.

3.3. Comparison with other models

Fig. 8 shows the comparison between our model ($\tau_n = 2.5 \times 10^{-11}$ s, and $v_s = 8.2 \times 10^6$ cm/s), Kroemer's model (infinite saturation velocity and infinite recombination lifetime), and Suzuki's model (finite saturation velocity (i.e., $v_s = 8.2 \times 10^6$ cm/s) and finite recombination lifetime) for trapezoidal Ge profile with doping of 5×10^{19} cm^{-3} and $\mathrm{Ge}(W) = \mathrm{Ge}(X_T) = 7\%$. It is clear that for the typical value of saturation velocity and recombination lifetime, the saturation velocity degrades the base transit time more seriously than recombination lifetime.

4. Conclusions

In this paper, an analytical base transit time model of Si/SiGe HBTs considering minority carrier recombination lifetime and velocity saturation at base–collector junction of the multi-graded Ge base has been studied. Our results show the decreasing base recombination lifetime and the finite saturation velocity increase the base transit time. The optimum Ge profile of the base can be obtained for given Ge content at base–collector junction with a drift electric field over the central portion of base. This optimal Ge profile agrees with Winterton's and Rinaldi's structures and is also applied to modern HBT technology [19]. The serious degradation of base transit time can occur if the severe recombination yields a diffusion length smaller than the base width.

Acknowledgements

This work is partly supported by Electronic Research and Service Organization of Industrial Technology Research Institute, the Republic of China. One of the authors (S.T. Chang) would like to thank the UMC for its Engineer Training Project of Technology and Process Development.

Appendix A

The parameters (A, B, C, and D) of Eq. (13) are determined by boundary conditions with the continuous electron concentration and total current at interface X_T. After calculation, the parameters are given by

$$A = -A_0/\Delta \tag{A.1}$$

$$B = -B_0/\Delta \tag{A.2}$$

$$C = -C_0/\Delta \tag{A.3}$$

$$D = -D_0/\Delta \tag{A.4}$$

where

$$\Delta = ae - be - af + bf + bcg - bdg - ach + adh \tag{A.5}$$

$$A_0 = bl - al + gr - hr + afs - bfs + bdgs - adhs - bgv + ahv \tag{A.6}$$

$$B_0 = al - bl - gr + hr - aes + bes - bcgs + achs + bgv + ahv \tag{A.7}$$

$$C_0 = -bcl + bdl - er + fr + chr - dhr - bdes + bcfs + bev - bfv \tag{A.8}$$

$$D_0 = er - fr - crg + drg + acl + ades - aces - ad + aces - aev - acfs + afv \tag{A.9}$$

where

$$a = \left(\frac{v_s + D_{n2}r'_+ - \mu_{n2}E_2}{v_s}\right)e^{r'_+(W-x_T)},$$

$$b = \left(\frac{v_s + D_{n2}r'_- - \mu_{n2}E_2}{v_s}\right)e^{r'_-(W-x_T)}, \quad c = -e^{r_+X_T},$$

$$d = -e^{r_-X_T}, \quad e = D_{n1}r_+e^{r_+X_T} + \mu_{n1}E_1e^{r_+X_T},$$

$$f = D_{n1}r_-e^{r_-X_T} + \mu_{n1}E_1e^{r_-X_T}, \quad g = -r'_+D_{n2} + \mu_{n2}E_2,$$

$$h = -r'_-D_{n2} + \mu_{n2}E_2, \quad s = n(0) - \frac{n_{ie}^2(0)}{N_B}e^{A_1\mathrm{Ge}(0)/KT},$$

$$G = \frac{n_{ie}^2(0)}{N_B}e^{A_1\mathrm{Ge}(0)/KT}, \quad G_T = \frac{n_{ie}^2(0)}{N_B}e^{A_1\mathrm{Ge}(X_T)/KT},$$

$$v = -Ge^{\alpha_2(W-X_T)/KT} - G_T,$$

$$r = -G_Te^{\alpha_2(W-X_T)/KT}\frac{v_s - \mu_{n2}E_2 + D_{n2}\alpha_2}{v_s}, \quad \text{and}$$

$$l = D_{n2}\alpha_2\mathbf{G}_Te^{\alpha_2(W-X_T)/KT} - D_{n1}G\alpha_1e^{\alpha_1X_T/KT} - \mu_{n2}E_2G_T + \mu_{n_1}E_1\mathrm{Ge}^{\alpha_1X_T}.$$

References

[1] Patton GL, Iyer SS, Delage SL, Tiwari S, Stork JMC. Silicon–germanium-base heterojunction bipolar transistors by molecular beam epitaxy. IEEE Electron Dev Lett 1988;9:165–7.

[2] Jagannathan B, Khater M, Pagette F, Rieh J-S, Angel D, Chen H, et al. Subbanna Self-align SiGe NPN transistors with 285 GHz fmax and 207 GHz ft in a manufacturable technology. IEEE Electron Dev 2002;23:258–60.

[3] Rieh J-S, Jagannathan B, Chen H, Schonenberg KT, Angell D, Chinthakindi A, et al. SiGe HBTs with cut-off frequency of 350 GHz. IEDM Tech Dig 2002:771–4.

[4] John JP, Chai F, Morgan D, Keller T, Kirchgessner J, Reuter R, et al. Optimization of a SiGe:C HBT in a BiCMOS technology for low power wireless applications. BCTM Tech Dig 2002:193–6.

[5] Morikawa T, Soda M, Shioiri S, Hashimoto T, Sato F, Emura K. A SiGe single-chip 3.3 V receiver IC for 10 Gb/s optical communication systems. IEEE Solid-State Circuit Conference, 1999. p. 380–1.

[6] Schüppen A, Erben U, Gruhle A, Kibbel H, Schumacher H, König U. Enhanced SiGe heterojunction bipolar transistors with 160 GHz f_{max}. IEDM Tech Dig 1995: 743–6.

[7] Joseph AJ, Cressler JD, Richy DM, Jaeger RC, Harame DL. Neutral base recombination and its influence on the temperature dependence of early voltage and current gain-early voltage product in UHV/CVD SiGe heterojunction bipolar transistors. IEEE Trans Electron Dev 1997;44: 404–13.

[8] Shafi ZA, Gibbings CJ, Ashburn P, Post ICR, Tuppen CG, Godfrey DJ. The important of neutral base recombination in compromising the gain of Si/SiGe heterojunction bipolar transistors. IEEE Trans Electron Dev 1991;38:1973–6.

[9] Shafi ZA, Ashburn P, Post IRC, Robbins DJ, Leong WY, Gibbings CJ, et al. Analysis and modeling of the base currents of Si/$Si_{1-x}Ge_x$ heterojunction bipolar transistors fabricated in high and low oxygen content material. J Appl Phys 1995;78:2823–9.

[10] Kroemer H. Two integral relations pertaining to the electron transport through a bipolar transistor with a nonuniform energy gap in the base region. Solid-State Electron 1985;28:1101–3.

[11] Suzuki K, Nakayama N. Base transit time of shallow-base bipolar transistors considering velocity saturation at base–collector junction. IEEE Trans Electron Dev 1992;39:623–8.

[12] Mohammadi S, Selvakumar CR. Analysis of BJT's, pseudo-HBT's, and HBT's by including the effect of neutral base recombination. IEEE Trans Electron Dev 1994;41:708–1714.

[13] Cressler JD, Crabbé EF, Comfort JH, Stork JMC, Sun JYC. On the profile design and optimization of epitaxial Si- and SiGe-base bipolar technology for 77 K applications—Part II: circuit performance issues. IEEE Trans Electron Dev 1993;40:542–55.

[14] Song J, Yuan JS. Comments on "On the base profile design and optimization of epitaxial Si- and SiGe-base bipolar technology for 77 K application—part II: circuit performance issues". IEEE Trans Electron Dev 1997;44:915–7.

[15] Patri VS, Kumar MJ. Profile design considerations for minimizing base transit time in SiGe HBT's. IEEE Trans Electron Dev 1998;45:1725–31.

[16] Patri VS, Kumar MJ. Novel Ge-profile design for high-speed SiGe HBTs: modeling and analysis. IEE Proc Circ Dev Syst 1999;146:291–6.

[17] Winterton SS, Peters CJ, Tarr NG. Composition grading for base transit time minimization in SiGe-base heterojunction bipolar transistors. Solid-State Electron 1993;36: 1161–4.

[18] Rinaldi P, Rinaldi N. Composition grading for base transit time minimization in HBTs: an analytical approach. Solid-State Electron 1997;41:59–66.

[19] Böck J, Meister TF, Knapp H, Zöschg D, Schäfer H, Aufinger K, et al. SiGe bipolar technology for mixed digital and analogue RF applications. IEDM Tech Dig 2000;2:745–8.

[20] Swirhum SE, Kwark YH, Swanson RM. Measurement of electron lifetime, electron mobility and band-gap narrowing in heavily doped p-type silicon. IEDM Tech Dig 1986:24–7.

[21] Suzuki K. Optimum base doping profile for minimum base transit time. IEEE Trans Electron Dev 1991;38:2128–33.

[22] Richey DM, Cressler JD, Joseph AJ. Scaling issues and Ge profile optimization in advanced UHV/CVD SiGe HBT's. IEEE Trans Electron Dev 1997;44:431–40.

[23] Thornber KK. Relation of drift velocity to low field mobility and high field saturation velocity. J Appl Phys 1979;51:2127–36.

[24] Krstelj ZM, Venkataraman V, Prinz EJ, Sturm JC, Magee CW. Base resistance and effective bandgap reduction in n–p–n Si/$Si_{1-x}Ge_x$/Si HBT's with heavy base doping. IEEE Trans Electron Dev 1996;43:457–65.

[25] Slotboom JW, Graaff HCD. Measurements of bandgap narrowing in Si bipolar transistors. Solid-State Electron 1976;19:857–62.

[26] Ershov M, Ryzhii V. High-field electron transport in SiGe alloy. Jpn J Appl Phys 1994;33(Part 1):1365–71.
[27] Bufler FM, Graf P, Meinerzhagen B, Adelin B, Rieger MM, Kibbel H, et al. Low- and high-field electron-transport parameters for unstrained and strained $Si_{1-x}Ge_x$. IEEE Electron Dev Lett 1997;18:264–6.
[28] Overstraeten RJV, Deman HJ, Mertens RP. Transport equation in heavy doped silicon. IEEE Trans Electron Dev 1973;20:290–8.